

## STOCHASTIC MODELS OF MEMRISTIVE BEHAVIOR

P.F. GÓRA<sup>†</sup>, EWA GUDOWSKA-NOWAKInstitute of Theoretical Physics  
andMark Kac Complex Systems Research Center  
Jagiellonian University, Łojasiewicza 11, 30-348 Kraków, Poland*Received 30 November 2024, accepted 11 February 2025,  
published online 20 February 2025*

Under normal operations, memristive devices undergo variability in time and space and have internal dynamics. Interplay of memory and stochastic signal processing in memristive devices makes them candidates for performing bio-inspired tasks of information transduction and transformation, where intrinsic random behavior can be harnessed for high performance of circuits built up of individual memory storing elements. The paper discusses models of single memristive devices exhibiting both — dynamic hysteresis and Stochastic Resonance, addressing also the cooperative effect of correlated noises acting on the system and occurrence of dirty hysteretic rounding.

DOI:10.5506/APhysPolB.56.2-A1

**1. Introduction**

The memristor, or the resistor with a memory, was first proposed by Chua in [1] as a “missing circuit element”. The original idea has been further extended [2] to memristive systems (otherwise named resistance-switching memory cells) and has gradually attracted interest from researchers and engineers, until the first actual memristor was reported to have been constructed in 2008 in HP Labs [3]. That incident brought about an explosion of attention in the field of theoretical frameworks and fabrication techniques, both intended to devise and construct electronic memory structures. There is a discussion whether true memristors, exhibiting the direct flux-charge interaction, exist. A discovery of such a device was reported in Ref. [4], but this research was met with much criticism [5], and has been later withdrawn. Usually, memristive devices are described in terms of deterministic mathematical models in which a key element is the existence of a pinched hysteresis loop [6, 7]. This feature of new components exhibiting memory

---

<sup>†</sup> Corresponding author: [pawel.gora@uj.edu.pl](mailto:pawel.gora@uj.edu.pl)

storage captured special interest of the communities focused on information and communication technologies, and found applications in areas such as unconventional, neuromorphic computing [5, 8], machine learning, models of the brain, and many others; see Refs. [9–12].

Memristive devices are resistors exhibiting the effect of “memory” or hysteretic behavior in response to external field or driving, and have been shown to emulate well functions of biological synapses. An intriguing concept in the field is neuron-like synchrony and performance of circuits built of elementary memristive units. Significant progress in understanding networks of memristive elements has been achieved recently in Ref. [13]. In addition, it has been strengthened that real (physical) memristive systems may significantly differ from their model counterparts; see Refs. [14–16] for a comprehensive review

$$\frac{d\mathbf{x}}{dt} = F(\mathbf{x}, u), \quad (1a)$$

$$y = H(\mathbf{x}, u) \cdot u. \quad (1b)$$

Here  $\mathbf{x}$  is a vector of internal states.  $F$  must be continuous for the solution to Eq. (1a) to exist. If  $\mathbf{x}$  is actually a vector, not a scalar, then  $F$  is also a vector function. The system has a memory, as the present-time values of  $y$  depend, via  $\mathbf{x}$ , on past values of  $u$ . This is the most general model of a memristive system [9]. One defines a specific, particular system by providing detailed information on  $\mathbf{x}$  and specifying the functions  $F$  and  $H$ . If the pair  $(y, u)$  is interpreted as current-voltage,  $(I, V)$ , we have a voltage-driven memristive system.

All the memristive systems discussed so far are assumed to be clean, or free of random perturbations. In reality, all systems are perturbed and can be modeled in terms of stochastic processes, representing the inner fluctuations in the systems or in their outer environments. These fluctuations are termed noise and traditionally are described by Gaussian White Noise (GWN) if they represent equilibrium fluctuations; sometimes memristive devices of this kind are called “stochastic” [17]. Usually, the effects of fluctuations are destructive as they blur or altogether destroy a coherent response of a system. However, sometimes fluctuations, or noises, can act constructively. Stochastic Resonance (SR) is the best-known phenomenon of this kind. In SR, noise and a dynamical system act together to reinforce a periodic signal [18–20]. The SR seems to be ubiquitous and has been claimed “an inherent property of rate-modulated series of events” [21, 22]. Several measures to quantify SR have been proposed [23]; we are going to use the most popular one, namely, the Signal-To-Noise Ratio (SNR) throughout this paper

$$\text{SNR} = 10 \log_{10} \frac{P_{\text{peak}}}{P_{\text{background}}}. \quad (2)$$

Here  $P_{\text{peak}}$  stands for the power spectrum at the peak corresponding to the external signal, and  $P_{\text{background}}$  is the extrapolated background. The interest in SR has now largely waned, but it still remains an important feature of many noise-perturbed systems. And surely enough, in memristive devices first a phenomenon of memory enhancement due to noise akin to SR has been reported in Ref. [24] and later a genuine SR in metal-dioxide memristors has been investigated in Ref. [25]. In addition, a model of stochastic resistance jumps in memristive devices, not leading to SR, has been recently discussed in Ref. [26].

Interestingly, effects similar to that of memristive devices, have been observed in voltage-activated ion channels [21, 27–29]. Ion channels, while not quite equivalent to memristive devices, share many of their features: the current passing through an ion channel may depend on history and display hysteretic behavior, and gating dynamics governed by low- and high-conductance states have been shown to exhibit stochastic resonance [21]. Hysteresis and memory effects are also important in such diverse contexts as social systems [30], security devices [31], and many others that are too numerous to cite them here.

Notwithstanding previous works on the constructive role of noises in nonlinear memristive systems [14, 24, 25], here we aim to discuss model systems where the quantitative analysis of memristic behavior is carried out within the framework of single- and multiple-well models of voltage-driven switching in conductance. In particular, double-well stochastic models of that type mimic the Kramers theory of activated rate processes and have been successfully applied to the analysis of the hysteresis phenomenon in the conductance of voltage-sensitive ion channels [28, 29, 32–34]. The other class of models discussed here involve single-well potentials with correlated multiplicative and additive noises [35–37]. They are not *directly* related to the double-well model, they just provide another example of constructive effects of noises on memristive systems. These models belong to the general (1) class, with the internal parameter  $\boldsymbol{x}$  being the dynamic conductance of the system, dubbed memductance in this context. It will be demonstrated that incorporating fluctuations enhances current passing through the memristive device, thus showing a typical for the SR scenario, amplification of a (weak) signal by noise.

## 2. Dynamic memory in voltage gated channels

Ion channels are transmembrane, pore-forming proteins which regulate ionic currents through the cell membrane and undergo conformation deformations under environmental (temperature, electric field, pressure) changes. At the level of a single channel, the gating process which changes perme-

ability of ions in response to voltage change across the cell membrane incorporates also local conformational variations of the constituting proteins. Hysteresis, termed otherwise “mode shift” in ion channels is a phenomenon in which a conductance loop arises in delayed response to voltage change, thus exhibiting a memory effect. Such hysteretic current-voltage characteristics has been detected in various biological channels [38–40] and the physiological significance of the phenomenon has been debated over the years [21, 34]. When the voltage varies sufficiently slowly, the protein constituent of the channel has enough time to adjust its conformation to the instantaneous value of the voltage. As a consequence, the ion current through the channel is independent of the prehistory, and hence no hysteresis is observed. On the other hand, when the period of the voltage change is much shorter than the characteristic protein relaxation time, the protein molecule cannot follow fast variations of the voltage and adapts only to its average value. As a consequence, the current through the channel becomes again independent of the former history, and the hysteresis loop collapses to a single line. Altogether, the loop area first grows monotonically with the frequency of voltage change, reaches a maximum, and disappears as the frequency tends to infinity. In models of a voltage-gated ion channel characterized by two states (open and closed), conductance  $G(t)$  corresponds to the probability  $P_O(t)$  of finding the channel in an open state [21, 32, 34]. For  $N$  uncorrelated channels, the time-dependent conductance obeys

$$G(t) = N [g_C + (g_O - g_C) P_O(t)] , \quad (3)$$

where  $g_i$  stands for the conductance of an individual channel in state  $i$ . Time evolution of  $G(t)$  is governed by combination of Eq. (3) and the rate equation

$$\frac{dP_O(t)}{dt} = -k_O(t)P_O(t) + k_C(t)[1 - P_O(t)] \quad (4)$$

in which the kinetic rates  $k_O(t) = k_O^* \exp[\alpha V(t)]$ ,  $k_C(t) = k_C^* \exp[-\beta V(t)]$  are voltage-dependent and describe stochastic transitions between open and closed states. The memristive equation of the ion channel is then

$$I(t) = G(P_O(t), V(t), t) V(t) , \quad (5)$$

where, in general, the conductance may be voltage-dependent. In real channels, the voltage sensitivity is determined by a corresponding set of charged residues that react to changes in voltage potential, promoting conformational changes of the protein that, in turn, generate a discrete change of conductance [21, 34, 41].

### 3. An asymmetric double-well

The free energy defines the work required to move from one region to another in phase space, such as *e.g.* between conformational states of a protein, or a channel operating between states of different conductance. In a recent study of the time-dependent anion channel VDAC [41], response to the trans-membrane potential in the form of gating to low/high-conductance states was analyzed by performing atomistic molecular dynamics studies. By choosing an appropriate collective “reaction coordinate” (be it *e.g.* conductance  $G$ ), histograms of configurational states can be assembled and probability density of states  $P(G)$  defined, see Fig. 1. From the latter, the free energy profiles can be estimated as  $V_{\text{eff}}(G) = -k_{\text{B}}T \ln P(G)$ .

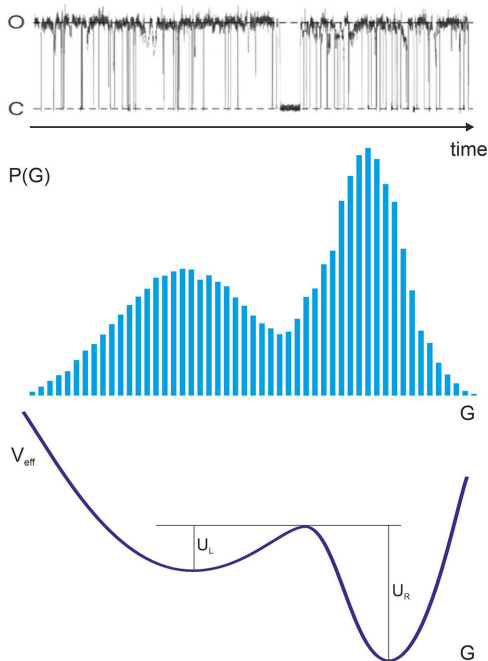


Fig. 1. Exemplary traces of a channel activity recorded at various conductance levels (C — closed state, O — open state) and histograms of conducting states derived from them (presented below the signal). Bottom: an asymmetric effective potential (free energy extracted from the stationary distribution) as  $-k_{\text{B}}T \ln(P(G))$ .

Our first model refers to such an approach and assumes the energy landscape of the channel gating in the form of the two well asymmetric (tilted) potential. Interestingly, a similar double-well potential has been experimentally observed in a virtual memristive device based on yttria stabilized zirconia film [42].

In our model, time changes in conductance follow then an overdamped motion in a potential, possessing two minima, with respective depths  $U_L, U_R$ . The particular shape of the potential is of lesser importance, but for the purpose of this research, the following potential has been used:

$$V(G) = \frac{1}{4}(G-2)^4 - \frac{1}{2}(G-2)^2 - \frac{1}{8}(G-2), \quad (6)$$

where  $G$  is the memory-dependent conductance (memductance) of the system. Such a configuration may be achieved by carefully doping a semiconductor. The equation of motion is

$$\dot{G} = -\frac{dV}{dG} + V_1 \cos \omega t + \sigma \xi(t), \quad (7)$$

and the associated current is

$$I(t) = G(t) \cdot V_1 \cos(\omega t), \quad (8)$$

where  $\xi$  is a Gaussian White Noise and  $\sigma$  represents its intensity. The amplitude  $V_1$  is too small to drive the particle over the barrier. In this research,  $V_1 = 0.2$  and  $\omega = 2\pi$ . In the absence of the external voltage,  $V_1 = 0$ , the escape from a potential well forms a classic Kramers problem. Therefore, the ratio of dwelling times in the right and left potential wells is

$$\tau_R/\tau_L \sim \exp\left(\frac{U_R - U_L}{\sigma}\right). \quad (9)$$

We assume that the system starts in states of low conductance (within the left potential well). Without the noise, the memductance would always remain there, but thanks to the noise, it may cross the barrier and increase the current (8) transmitted by the system. Once in the right well and provided the noise is *not* very large, the system has a tendency to stay there and perform noisy oscillation around the deeper minimum.

System (7) has been solved numerically with the Euler–Maruyama method and a timestep  $\Delta t = 1/256$ . For the purpose of calculating SNR, trajectories have been averaged over 512 realizations for every single value of  $\sigma$ . For a very weak noise,  $\sigma = 0.01$ , the memductance displays oscillations in the left potential well. However, consecutive minima and maxima are shifted due to the noise, and instead of a clear hysteresis loop, we can see a collection of overlapping loops. For larger noise intensities,  $\sigma = 0.5$  and  $\sigma = 0.75$ , the system crosses to the right potential well and spends most of its time there. This means an increase of the memductance, but instead of a clear hysteresis loop, we obtain a combination of many overlapping, individual loops, bearing the impression of a “dirty hysteresis”, see Fig. 2.

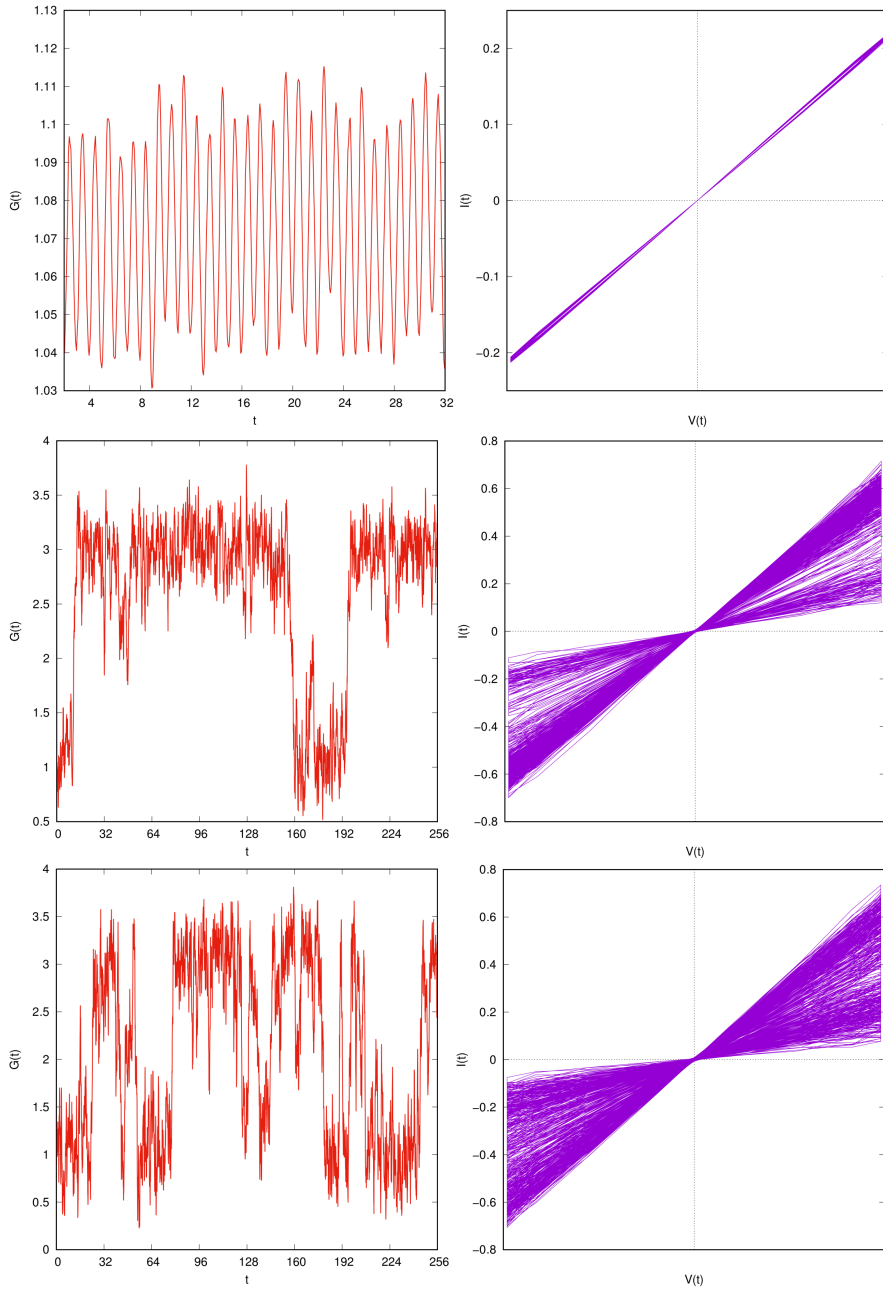


Fig. 2. Example trajectories (left column) and their corresponding hysteresis loops (right column) for system (7). Noise intensities are, top to bottom,  $\sigma = 0.01$ ,  $\sigma = 0.5$ , and  $\sigma = 0.75$ .

For even larger intensities of the noise, system (7) ceases to see the fine structure of the potential and the memductance performs a random walk over all accessible range. This leads to a peculiar behavior of the SNR, see Fig. 3. For very small noises, the system performs nearly perfect oscillations in the left potential well and the SNR is large. As the noise increases, it gradually destroys the oscillations and the SNR decreases, finally reaching a minimum. After that, the constructive role of noise kicks in, helping the memductance to cross to the right potential well in phase with the external voltage. The SNR reaches a maximum and a Stochastic Resonance is observed. However, for even larger values of the noise, the SNR displays a rather strange behavior: unlike in the regular SR, the SNR does not drop to zero, but reaches a plateau that extends up to unphysically large intensities of the noise.

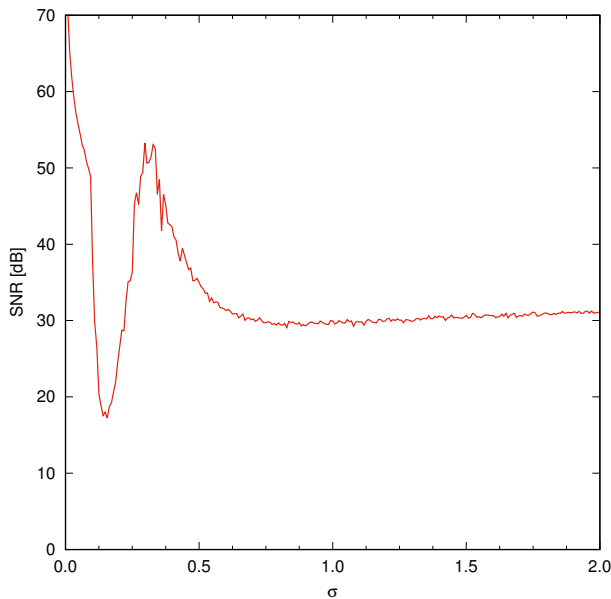


Fig. 3. The Signal-To-Noise Ratio in the system (7) as a function of the GWN intensity.

This last phenomenon requires, perhaps, some attention. The power spectrum of current (8) is related through the Wiener–Khinchin theorem to the autocorrelation  $\langle I(t)I(t+t') \rangle = \langle G(t)G(t+t') \rangle \cos \omega t \cos \omega(t+t')$ . If the noise is very large, the memductance  $G(t)$  discontinues to see details of the potential and is smeared over all accessible range with  $\langle G(t) \rangle = \tilde{G} \neq 0$  due to the asymmetry of the potential with respect to sign reversal.  $\gamma(t) = G(t) - \tilde{G}$  is a random variable satisfying  $\langle \gamma(t) \rangle = 0$ . The existence

of  $\langle \gamma(t)\gamma(t+t') \rangle$  is guaranteed by the fact that the process is driven by a GWN. Therefore,

$$\langle G(t)G(t+t') \rangle = \langle \gamma(t)\gamma(t+t') \rangle + \tilde{G}^2. \quad (10)$$

The presence of  $\tilde{G}^2 \neq 0$  is responsible for the plateau in the SNR.

#### 4. Harmonic well with correlated noises

The other model discussed in this paper relates to the Linear Stochastic Resonance (LSR) [35]. LSR is a kind of SR where a signal-enhancing effect arises from cooperation between a linear transmitter and two GWNs acting on it, one multiplicative, or parametric, the other additive. Instead of (6), we take

$$V(G) = \frac{1}{2}aG^2 - V_0G. \quad (11)$$

With the absence of any noises, this system leads to a time-delay behavior. We now perturb the model by two GWNs: A multiplicative,  $\xi(t)$  with an intensity  $p$ , and an additive,  $\xi_a(t)$  with an intensity  $q$ , noises. The evolution equation for the memductance is

$$\dot{G}(t) = -(a + p\xi(t))G + V_0 + q\xi_a(t) + V_1 \cos(\omega t + \phi), \quad (12)$$

where  $\phi$  is a random initial phase of the signal and we take the Ito interpretation of the multiplicative noise. Since both noises originate in the same physical system in a thermal equilibrium interacting with system (11), it is reasonable to assume that they are correlated

$$\langle \xi(t)\xi_a(t') \rangle = c\delta(t-t'), \quad -1 \leq c \leq 1. \quad (13)$$

The noises represent interactions with a multitude of unobserved degrees of freedom. Note that while equation (12) is formally linear, a multiplicative (nonlinear) coupling between the stochastic process and the observed memductance reflects the presence of a “hidden” nonlinearity.

We may represent the additive noise  $\xi_a(t)$  as a combination of two independent GWNs

$$\xi_a(t) = c\xi(t) + \sqrt{1-c^2}\eta(t), \quad (14)$$

with  $\langle \xi(t)\eta(t') \rangle = 0$ , leading to

$$\begin{aligned} \dot{G} = & -(a + p\xi(t))G + V_0 + qc\xi(t) + q\sqrt{1-c^2}\eta(t) \\ & + V_1 \cos(\omega t + \phi). \end{aligned} \quad (15)$$

System (15) has been discussed in Ref. [35]. The formal solution with  $G(0) = 0$  is

$$G(t) = \int_0^t e^{-a(t-t')} \exp \left[ -p \int_{t'}^t \xi(t'') dt'' \right] \times \left( V_0 + qc \xi(t') + q\sqrt{1-c^2} \eta(t') + V_1 \cos(\omega t' + \phi) \right) dt'. \quad (16)$$

This solution has a well-defined mean if

$$a - \frac{1}{2}p^2 > 0, \quad (17)$$

and a variance if a stronger condition

$$a - p^2 > 0 \quad (18)$$

holds. In this case, for  $V_1 = 0$ , the solution is

$$\langle G(t) \rangle \xrightarrow{t \rightarrow \infty} G_\infty = \frac{V_0 - \frac{1}{2}cpq}{a - \frac{1}{2}p^2}, \quad (19)$$

and the variance asymptotically takes the form

$$\langle G^2(t) \rangle - \langle G(t) \rangle^2 \xrightarrow{t \rightarrow \infty} D = \frac{4V_0^2 p^2 - 8aV_0 cpq + (4a^2 - 4a(1-c^2)p^2 + (1-c^2)p^4)q^2}{2(a-p^2)(p^2-2a)^2}. \quad (20)$$

For  $V_1 \neq 0$ , we can calculate the correlation function

$$\langle G(t)G(t+\tau) \rangle - \langle G(t) \rangle^2 \xrightarrow{t \rightarrow \infty} \frac{V_1^2 \cos(\omega\tau)}{2 \left[ \left( a - \frac{1}{2}p^2 \right)^2 + \omega^2 \right]} + \left[ \frac{V_1^2 p^2}{4(a-p^2) \left[ \left( a - \frac{1}{2}p^2 \right)^2 + \omega^2 \right]} + D \right] e^{-(a-\frac{1}{2}p^2)\tau} \quad (21)$$

where now the braces additionally represent averaging over the initial phase of the signal.

The most interesting feature of the above solution is that if

$$V_0 p - acq = 0, \quad (22)$$

then for  $c \neq 0$ , the variance  $D$  reaches a minimum. This is so because with the condition of (22) satisfied, Eq. (15) can be written as

$$\dot{G} = -(a + p\xi(t))(G - V_0/a) + q\sqrt{1 - c^2}\eta(t) + V_1 \cos(\omega t + \phi). \quad (23)$$

As we can see, part of the additive noise translates only to a shift in the equilibrium solution and  $G_\infty = V_0/a$ , as in the deterministic case. We can think of the parameters of the potential,  $a$  and  $V_0$ , and the intensity of the multiplicative noise,  $p$ , as fixed, but suppose we can control the intensity of the additive noise,  $q$ . We can see that by manipulating  $q$ , we can make the correlated part of the additive noise to act in unison with the multiplicative part. Their combined effect results just in shifting of the equilibrium value of  $G$ . If the condition of (22) is satisfied, a contribution from the correlated part of the additive noise is eliminated, reducing the variance,  $D$ , and lowering the noise background, leading to an increase in the Signal-To-Noise ratio, *cf.* (2).

Furthermore, if  $c = 1$  with condition (22) satisfied, the additive noise is eliminated altogether. Without the external signal,  $V_1 = 0$ , the formal solution (16) now reads

$$G(t) = \frac{V_0}{a} + \left( G(0) - \frac{V_0}{a} \right) \exp \left[ -at - p \int_0^t \xi(t') dt' \right], \quad (24)$$

where  $G(0)$  is the initial value of the memductance. If the multiplicative noise is not too strong, *cf.* Eq. (18), almost all realizations asymptotically approach  $G_\infty = V_0/a$ . The variance asymptotically vanishes,  $D \rightarrow 0$ , and the device behaves as a noise-free resistor. When  $V_1 \neq 0$ ,  $c = 1$ , and with the condition of (22) satisfied, the solution is still noisy, but minimally so for a given amplitude of the multiplicative noise,  $p$ , see Fig. 4. A similar reasoning holds for  $c = -1$ .

Because  $D$  enters the expression for the correlation function (21), minimizing  $D$  corresponds to optimizing the current (8) with respect to the external signal with amplitude of the multiplicative noise,  $p$ , fixed. We have solved Eq. (15) numerically with the Euler–Maryuama scheme with a timestep  $\Delta t = 1/256$ . Numerical power spectra have been averaged over 128 realizations of the noises. Results for the model (15) are presented in Figs. 5 and 6 for different values of the multiplicative noise amplitude,  $p$ . For  $c = 1$ , a clear stochastic resonance is visible. The stochastic resonance persists for

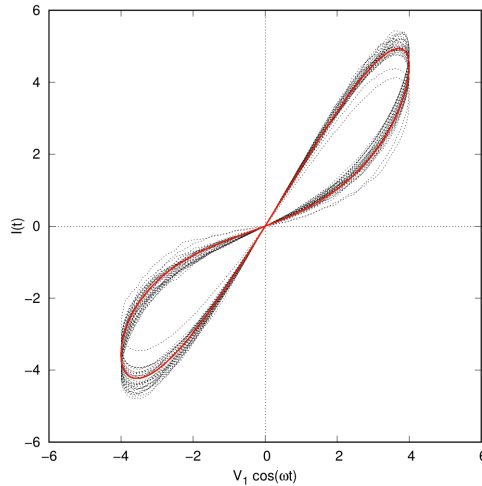


Fig. 4. Broken line — the noisy hysteresis loop for  $p = 0.25$ ,  $c = 1$  and with the condition of (22) satisfied. The other parameters are  $V_0 = 1$ ,  $a = 1$ ,  $V_1 = 4$ ,  $\omega = 2\pi$ . The colored line shows the clean hysteresis loop corresponding to the same set of parameters.

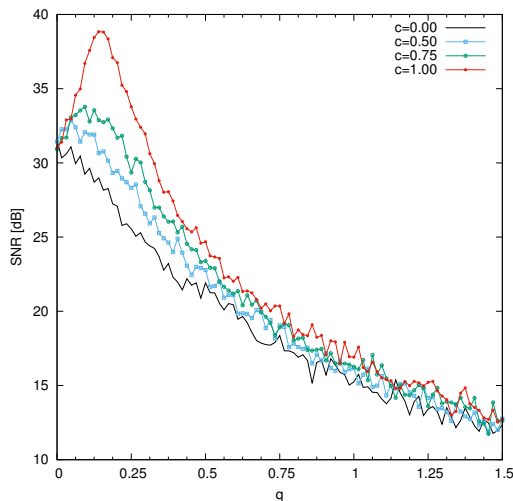


Fig. 5. Numerically obtained Signal-To-Noise ratio as a function of the intensity of the additive noise,  $q$ , for different values of the correlation coefficient,  $c$ . The multiplicative noise intensity  $p = 0.15$ . All other parameters as in Fig. 4.

all  $c \neq 0$ , but for small values of  $c$ , SR is drowned by numerical fluctuations. For uncorrelated additive and multiplicative noises,  $c = 0$ , the stochastic resonance vanishes altogether and the resulting hysteresis loop becomes much more irregular due to the maximization of the additive noise. Trajectories

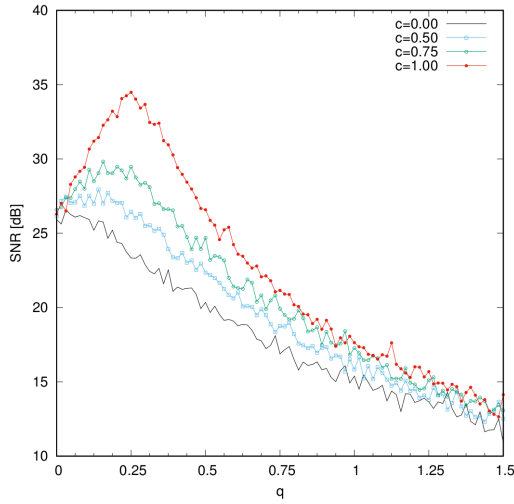


Fig. 6. The same as Fig. 5, but with the multiplicative noise intensity  $p = 0.25$ .

representing negative memductances are clearly visible, as shown in Fig. 7. Negative memductances represent a paradoxical behavior with current passing against the voltage. We can see that too large values of noise intensities, when not mitigated by mutual correlations, can lead to unphysical behavior of our model memristive system.

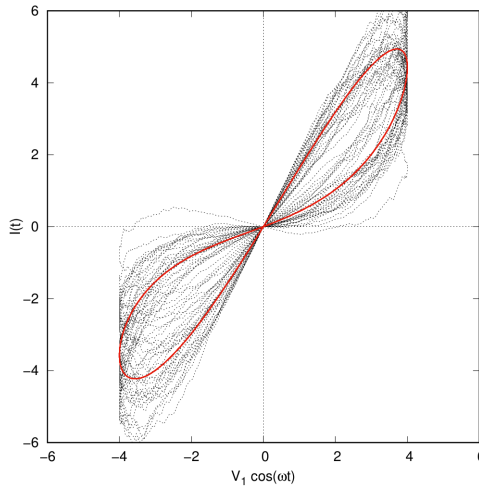


Fig. 7. The same as in Fig. 4, but for  $c = 0$  and  $p = q = 0.25$ .

Interestingly, for both amplitudes of the noises,  $p$  and  $q$ , fixed, for  $c \neq 0$ , the resonance condition (22) can still be reached by changing  $V_0$ . This, however, means changing the shape of the noise-free hysteresis as well.

### 5. Higher-order monostable wells

Results for the LSR can be generalized to higher-order monostable potential wells. Suppose that instead of relaxing in a harmonic well, the particle whose position represents the memductance relaxes in a potential  $\frac{1}{2n}G^{2n}$ ,  $n = 2, 3, \dots$ . We now have

$$\begin{aligned} \dot{G} = & -(a + p\xi(t))G^{2n-1} + V_0 + qc\xi(t) + q\sqrt{1-c^2}\eta(t) \\ & + V_1 \cos(\omega t + \phi) \end{aligned} \quad (25)$$

and for  $c \neq 0$ , with the condition (22) satisfied,

$$\begin{aligned} \dot{G} = & -(a + p\xi(t)) (G^{2n-1} - V_0/a) + q\sqrt{1-c^2}\eta(t) \\ & + V_1 \cos(\omega t + \phi). \end{aligned} \quad (26)$$

The intensity of the multiplicative noise,  $p$ , cannot be arbitrary large as the system would become divergent. Unlike in the linear case, *cf.* Eq. (18), the maximal intensity can be assessed only numerically; it is always smaller than in the linear case.

Substituting  $y = G - (V_0/a)^{1/(2n-1)}$  we get

$$\dot{y} = -(a + p\xi(t))yW(y) + q\sqrt{1-c^2}\eta(t) + V_1 \cos(\omega t + \phi), \quad (27)$$

where

$$W(y) = \sum_{l=0}^{2(n-1)} \binom{2n-1}{l+1} y^l (V_0/a)^{1-\frac{l+1}{2n-1}} \quad (28)$$

is a polynomial of the order of  $2(n-1)$ . As we can see, correlations between the multiplicative and additive noises again result in shifting of the equilibrium solution and reducing the additive noise. If  $c = \pm 1$  and the resonance condition (22) is satisfied, the additive noise is eliminated completely.

If there is no external signal,  $V_1 = 0$ , and the additive noise is eliminated, Eq. (27) is formally solved as

$$\int \frac{dy}{yW(y)} = -at - p \int_0^t \xi(t') dt'. \quad (29)$$

For  $n = 2$ , the integral on the left-hand side of Eq. (29) can be carried out analytically, but even then the resulting expression cannot be solved for

$y$  explicitly. In general, Eq. (25) can be solved only numerically. Due to the nonlinear character of Eqs. (25), (27), a solution for  $V_1 \neq 0$  cannot be represented as a convolution of the free solution and the external forcing, as in the linear case discussed above. However, as the integral in (29) contains a logarithmic term, we expect that the condition of (18) needs to be satisfied for the variance of the solution to exist. Numerical experiments confirm this intuition.

We have solved Eq. (25) numerically for the quartic ( $n = 2$ ) potential. The solutions display a hysteresis loop, as expected. Numerical experiments show that the nonlinearity significantly reduces the range of parameters for which negative memductances do not appear. Figure 8 shows a hysteresis loop in a resonant case.

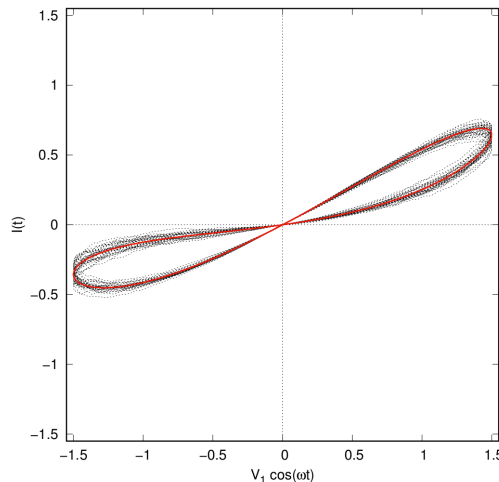


Fig. 8. Broken life — the noisy hysteresis loop for the quartic well, (25) with  $n = 2$ ,  $c = 1$  and the condition of (22) is satisfied. Parameters are  $V_0 = 1$ ,  $a = 1$ ,  $p = 0.15$ ,  $V_1 = 1.5$ ,  $\omega = 2\pi$ . The colored line shows the clean hysteresis loop corresponding to the same set of parameters. (Note a different scale as compared to Fig. 4.)

Because with the amplitude of the multiplicative noise equal  $p = 0.25$  as in Fig. 4 leads to negative memductances, we have used a smaller value of  $p = 0.15$  and the noisy hysteresis is less blurred. Figure 9 shows the SNR. In a quartic well, the stochastic resonance is even stronger than in the LSR. SR is present for all  $c \neq 0$ , but for small values of  $c$  it is hardly visible.

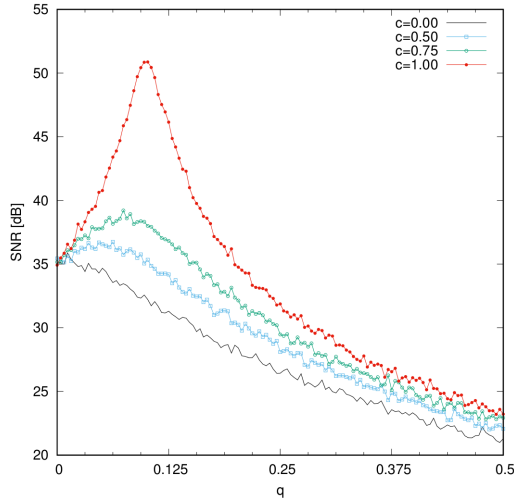


Fig. 9. Numerically obtained Signal-To-Noise Ratio as a function of the intensity of the additive noise,  $q$ , in the model of (25), for different values of the correlation coefficient,  $c$ . Other parameters as in Fig. 8.

## 6. Conclusions

In this paper, we have addressed the effect of noise on signal transmission in model memristive devices. On the one hand, side miniaturization of electronic processors allows for integration of many circuit elements per unit area and lowers the driving voltage, on the other hand, it naturally makes the systems vulnerable to thermal,  $1/f$ , shot and external, environmental noises. At the same time, based on theoretical approaches and experimental considerations, it has been documented that better endurance of signal transmission in natural and artificial systems can be achieved by understanding the source and making use of inherent temporal fluctuations in resistive devices. Contemporary methods used in the design of artificial signal transferring systems try to mimic information processing mechanisms of living organisms and to emulate states of conductance of neuron synapses by analyzing stochastic response of neuron-like units and networks. Taken from that perspective, the Stochastic Resonance phenomenon may serve as an event optimizing performance of a system in the presence of noise, alike hearing or visual sensations have been shown to be amplified [20, 43–45] by interference of weak signals and temporal fluctuations.

Theoretical models as investigated here were mostly motivated by studies on protein channels and synthetic micropores in metal-organic frameworks (MOF) [46–50] where hysteretic behavior has been observed. In particular, authors of Ref. [48] presented extensive experimental studies of the class

of iono-neuromorphic biomolecular memristor, whose switching mechanism and ionic transport resembles biosynapses. The physical mechanism has been modeled by running simulations based on Eq. (5) where the conductance was assumed to depend on the number of pores per unit area. In turn, Catacuzzeno *et al.* used a model of voltage-dependent potassium channel based on the description of the voltage sensor represented as a Brownian particle diffusing in multimodal energy profile related to the change of the sensor position in the channel and MD simulations of the conformation variations of the channel protein. Similar abstraction of the gating process analyzed by stochastic modeling has been addressed by Metri *et al.* [49]. Notably, in those models, hysteresis in gating has been attributed to the difference in energy between conformations of the channel represented by either discrete or continuous variations of  $G(V(t), t)$ .

Our research shows that a conceptually very simple system of a particle relaxing in a potential well can model the memristive behavior under the influence of noise. We have discussed two kinds of models which, in addition to the memristive behavior, display a Stochastic Resonance. In the model involving a tilted double-well potential we observe a “dirty hysteresis” consisting of multiple overlapping hysteresis loops, reminiscent of hysteretic rounding observed in plastic or disordered materials. In the model involving a monostable well subject to correlated multiplicative and additive noises — a harmonic well that can be solved analytically and its generalisations to higher-order wells — a blurred hysteresis is observed, much as in the case of hysteresis loops observed in voltage-activated ion channels [27–29]. This highlights a previously unexpected connection between memristive systems and ion channels. Indeed, data presented in Fig. 1 that gave rise to our model double-well potential (6) resemble those obtained experimentally for a “virtual memristor” in Ref. [42]. The question remains how integration of such units in neuromorphic architecture will influence properties of the circuit and its performance in signal transduction.

We would like to thank Benjamin Lindner for a most helpful discussion. This work has been supported by the Priority Research Area SciMat under the programme Excellence Initiative — Research University at the Jagiellonian University in Kraków.

## REFERENCES

- [1] L. Chua, «Memristor — The missing circuit element», *IEEE Trans. Circuit Theor.* **5**, 507 (1971).
- [2] L. Chua, S.M. Kang, «Memristive devices and systems» *Proc. IEEE* **64**, 209 (1976).
- [3] D.B. Strukov, G.S. Snider, D.R. Stewart, R.S. Williams, «The missing memristor found», *Nature* **453**, 80 (2008).
- [4] F. Wang *et al.*, « $\Phi$  memristor: Real memristor found», *J. Appl. Phys.* **125**, 054504 (2019).
- [5] Y.V. Pershin, J. Kim, T. Datta, M. Di Ventra, «An experimental demonstration of the memristor test», *Physica E* **142**, 115290 (2022).
- [6] Y.V. Pershin, M. Di Ventra, «Memory effects in complex materials and nanoscale systems», *Adv. Phys.* **60**, 145 (2011).
- [7] L. Chua, «If it's pinched it's a memristor», *Semicond. Sci. Technol.* **29**, 104001 (2014).
- [8] Y.V. Pershin, M. Di Ventra, «A simple test for ideal memristor», *J. Phys. D: Appl. Phys.* **52**, 01LT01 (2018).
- [9] F. Caravelli, J.P. Carbajal, «Memristors for the Curious Outsiders», *Technologies* **6**, 118 (2018).
- [10] A.G. Radwan, M.E. Fouda, A.G. Radwan, M.E. Fouda, «On the mathematical modeling of memristor, memcapacitor and meminductor», *Springer International Publishing, Cham* 2015.
- [11] S. Battistoni *et al.*, «The Role of the Internal Capacitance in Organic Memristive Device for Neuromorphic and Sensing Applications», *Adv. Electron. Mater.* **8**, 2101319 (2022).
- [12] F.J. Alonso, D. Maldonado, A.M. Aguilera, J.B. Roldán, «Memristor variability and stochastic physical properties modeling from a multivariate time series approach», *Chaos, Solitons Fractals* **143**, 110461 (2021).
- [13] F. Caravelli, F.L. Traversa, M. Di Ventra, «The complex dynamics of memristive circuits: analytical results and universal slow relaxation», *Phys. Rev. E* **95**, 022140 (2017).
- [14] J.B. Roldán *et al.*, «Variability in Resistive Memories» *Adv. Intell. Syst.* **5**, 2200338 (2023).
- [15] Q. Wan, Y. Shi, «Neuromorphic Devices for Brain-Inspired Computing: Artificial Intelligence, Perception and Robotics», *Wiley*, 2022.
- [16] C.S. Hwang, «Prospective of Semiconductor Memory Devices: from Memory System to Materials», *Adv. Electron. Mater.* **1**, 1400056 (2015).
- [17] V.G. Karpov, D. Niraula, I.V. Karpov, R. Kotlyar, «Thermodynamics of Phase Transitions and Bipolar Filamentary Switching in Resistive Random-Access Memory», *Phys. Rev. Appl.* **8**, 024028 (2017).

- [18] R. Benzi, A. Sutera, A. Vulpiani, «The mechanism of stochastic resonance», *J. Phys. A: Math. Gen.* **14**, L453 (1981).
- [19] C. Nicolis, G. Nicolis, «Stochastic aspects of climatic transitions — additive fluctuations», *Tellus* **33**, 225 (1981).
- [20] L. Gammaitoni, P. Hänggi, P. Jung, F. Marchesoni, «Stochastic resonance», *Rev. Mod. Phys.* **70**, 223 (1998).
- [21] S.M. Bezrukov, I. Voydanoy, «Stochastic resonance in non-dynamical systems without response thresholds», *Nature* **385**, 319 (1997).
- [22] B. Dybiec, E. Gudowska-Nowak, «Lévy stable noise induced transitions: Stochastic resonance, resonant activation and dynamic hysteresis» *J. Stat. Mech.* **2009**, P05004 (2009).
- [23] M. Evstigneev, P. Reimann, C. Schmitt, C. Bechinger, «Quantifying stochastic resonance: theory versus experiment», *J. Phys.: Cond. Matt.* **17**, S3795 (2005).
- [24] A. Stotland, M. Di Ventra, «Stochastic memory: Memory enhancement due to noise», *Phys. Rev. E* **85**, 011116 (2012).
- [25] A.N. Mikhaylov *et al.*, *Chaos, Solitons Fractals* **144**, 110723 (2021).
- [26] V.A. Slipko, Y.V. Pershin, «Probabilistic model of resistance jumps in memristive devices», *Phys. Rev. E* **107**, 064117 (2023).
- [27] E. Gudowska-Nowak, B. Dybiec, H. Flyvbjerg, «Resonant effects in a voltage-activated channel gating», *Proc. SPIE* **5467**, 223 (2004).
- [28] H. Flyvbjerg, E. Gudowska-Nowak, P. Christophersen, P. Bennekou, «Modeling hysteresis observed in the human erythrocyte voltage-dependent cation channel», *Acta Phys. Pol. B* **43**, 2117 (2012).
- [29] S.M. Rappaport *et al.*, «Conductance hysteresis in the voltage-dependent anion channel», *Eur. Biophys. J.* **44**, 465 (2015).
- [30] K. Sznajd-Weron, A. Jedrzejewski, B. Kamińska, «Toward Understanding of the Social Hysteresis: Insights From Agent-Based Modeling», *Perspect. Psychol. Sci.* **2023**, 1 (2023).
- [31] R. Carboni, D. Ielemi, «Stochastic Memory Devices for Security and Computing», *Adv. Electron. Mater.* **5**, 1900198 (2019).
- [32] B. Lisowski, M. Żabicki, B. Dybiec, E. Gudowska-Nowak, «Entropy production and collective phenomena in biological channel gating», *Acta Phys. Pol. B* **50**, 911 (2019).
- [33] M.A. Pustovoi, A.M. Berezhovskii, S.M. Bezrukov, «Analytical theory of hysteresis in ion channels: Two-state model», *J. Chem. Phys.* **125**, 194907 (2006).
- [34] T. Andersson, «Exploring voltage-dependent ion channels *in silico* by hysteresis conductance», *Math. Biosci.* **226**, 16 (2010).
- [35] P.F. Góra, «The logistic equation and a linear stochastic resonance», *Acta Phys. Pol. B* **35**, 1583 (2004).
- [36] P.F. Góra, «Stationary distributions for a noisy logistic process», *Acta Phys. Pol. B* **36**, 1981 (2005).

- [37] P.F. Góra, «An exactly solvable nonlinear model: Constructive effects of correlations between Gaussian noises», *Physica A* **378**, 201 (2007).
- [38] E. Krueger *et al.*, «A model for the hysteresis observed in gating of lysenin channels», *Biophys. Chem.* **184**, 126 (2013).
- [39] L.M. Nowak, J.M. Wright, «Slow voltage-dependent changes in channel open-state probability underlie hysteresis of NMDA responses in  $Mg^{2+}$ -free solutions», *Neuron* **8**, 181 (1992).
- [40] P. Bennekou *et al.*, «Voltage activation and hysteresis of the non-selective voltage-dependent channel in the intact human red cell», *Bioelectrochem.* **62**, 181 (2004).
- [41] V.A. Ngo *et al.*, «The Single Residue K12 Governs the Exceptional Voltage Sensitivity of Mitochondrial Voltage-Dependent Anion Channel Gating», *J. Am. Phys. Soc.* **144**, 14564 (2022).
- [42] D.O. Filatov *et al.*, «Experimental investigations of local stochastic resistive switching in yttria stabilized zirconia film on a conductive substrate», *J. Stat. Mech.* **2020**, 024005 (2020).
- [43] A. Schilling, K. Tziridis, H. Schulze, P. Krauss, «The stochastic resonance model of auditory perception: A unified explanation of tinnitus development, Zwicker tone illusion, and residual inhibition», *Prog. Brain Res.* **262**, 139 (2021).
- [44] E. Simonotto *et al.*, «Visual Perception of Stochastic Resonance», *Phys. Rev. Lett.* **78**, 1186 (1997).
- [45] D.R. Chialvo, A. Longtin, J. Müller-Gerking, «Stochastic resonance in models of neuronal ensembles», *Phys. Rev. E* **55**, 1798 (1997).
- [46] C. Tilegenova, D.M. Cortes, L.G. Cuello, «Hysteresis of KcsA potassium channel's activation-deactivation gating is caused by structural changes at the channel's selectivity filter», *Proc. Natl. Acad. Sci. U.S.A.* **114**, 3234 (2017).
- [47] L. Catacuzzeno, L. Sforza, F. Franciolini, «Voltage-dependent gating in K channels: experimental results and quantitative models», *Pflügers Arch. — Eur. J. Physiol.* **472**, 27 (2020).
- [48] J.S. Najem *et al.*, «Memristive Ion Channel-Doped Biomembranes as Synaptic Mimics», *ACS Nano* **12**, 4702 (2018).
- [49] V. Metri, S. Ghatak, S. Raha, S.K. Sikdar, «Patch clamp data driven stochastic modeling and simulation of hTREK1 potassium ion channel gating» *Chem. Phys.* **516**, 182 (2019).
- [50] Z. Li, J. Turner, R.Q. Snurr, «Computational investigation of hysteresis and phase equilibria of n-alkanes in a metal-organic framework with both micropores and mesopores», *Commun. Chem.* **6**, 90 (2023).